International Symposium
On Turbulence and Shear Flow
Phenomena (TSFP-9)
June 30 - July 3, 2015 *Melbourne, Australia*

EFFECT OF EXTERNAL TURBULENCE ON A TURBULENT WAKE

Anikesh Pal and Sutanu Sarkar
Department of Mechanical and Aerospace Engineering
University of California San Diego
CA 92093
anpal@ucsd.edu, sarkar@ucsd.edu

ABSTRACT

Direct numerical simulations are performed to study the evolution of a $Re = 10,000$ axisymmetric wake under the influence of unforced external (background) turbulence. The external turbulence has an integral length scale 4 times larger than that of the wake turbulence in contrast to Pal & Sarkar (2015) where this ratio was approximately unity. Entrainment of background turbulence leads to a reduction of the wake defect velocity relative to the undisturbed wake. The reduction is significant even when the initial r.m.s of background turbulence is only $1-3\%$ of the body velocity, whereas a similarly strong reductions in the cases simulated by Pal & Sarkar (2015) required $5-7\%$ initial turbulence levels. This difference is attributed to external turbulence having a slower decay relative to wake turbulence in the present cases owing to the larger eddy-turnover time.

INTRODUCTION

The wake behind an axisymmetric body is a benchmark turbulent flow. Detailed investigations of axisymmetric turbulent wakes have been carried out using theory, experiment and simulations. Notably, the characteristics of turbulence in the far wake and the approach to self-similarity have received much attention. Uberoi & Freymuth (1970) experimentally studied the axisymmetric turbulent wake of a sphere at Re=4,000 to 15,0000 and reported the details of the turbulent energy balance in the dynamic self-similar region of the wake. Bevilaqua & Lykoudis (1978) found that, contrary to the equilibrium hypothesis of Townsend, different geometries with the same drag can have different self-preserving states. Wygnanski *et al.* (1986) concluded that the characteristic velocity and length scales in the wake do not exhibit self-similar behavior and are dependent on the initial conditions and the geometry of the wake generator. Subsequently, Johansson *et al.* (2003) used the equilibrium similarity approach to show that, depending on the upstream conditions, the axisymmetric wake width would either evolve as $r \sim x^{1/3}$ or $r \sim x^{1/2}$ based on infinite local Re or small local Re limits, respectively. However, a more recent numerical study by Redford *et al.* (2012) shows that the axisymmetric, temporally evolving wake reaches a self-similar state, albeit after a very long time, even when the initial conditions are varied.

Wakes of bodies often develop in the presence of external (background) turbulence, e.g propelled bodies, marine animals, wind turbines, and particles in multiphase flow. Much of our current knowledge regarding the evolution of axisymmetric unstratified wakes in the presence of external turbulence is derived from work related to multiphase particulate flows. Thus, the body Reynolds number $Re = UD/\nu \sim O(100-1000)$ was small, the turbulence integral length scale l_{int} was large relative to the body leading to $l_{int}/D \sim O(10-100)$, and the far wake was not measured in those studies. Here, U is the freestream velocity and D is the body diameter. The level of external turbulence measured by the normalized root mean square (r.m.s) of the streamwise velocity fluctuation, u'_{ext}/U, ranged from low to high values. Although our motivation is different, in particular, we study the intermediate-to-far wake properties as well as larger bodies with larger Re and $l_{int}/D \sim O(1)$, we briefly review the literature in that different regime in the following paragraph.

Wu & Faeth (1994) experimentally studied a sphere placed at the axis of turbulent pipe flow over the range, $Re = 135-1560$, and $u'_{ext}/U = 4\%$, making measurements up to $x/D \sim 20$. They found that, despite being turbulent, the wake has a self-preserving behavior with a laminar-like scaling law: the mean defect velocity, $U_0(x) \sim x^{-1}$, and the wake half width $r \sim x^{1/2}$. The x^{-1} scaling was attributed to a constant (radially and axially) turbulent eddy viscosity and the wake spread rate was found to increase with increasing level of external turbulence. Wu & Faeth (1995) explored stronger external turbulence levels (u'_{ext}/U up to 9%) finding that the wake decayed faster than x^{-1}, but did not further quantify the power law exponent. Bagchi & Balachandar (2004) performed DNS of flow past a sphere embedded in a frozen realization of homogeneous, isotropic turbulence. The level of free stream turbulence ($u'_{ext}/U = 10-25\%$) was high, and the sphere was relatively very small so that $l_{int}/D = 52-333$ and $Re = 50-600$. The wake, simulated until $x/D = 15$, was found to exhibit $U_0 \sim x^{-1}$ decay of the mean defect velocity and a wake spreading rate that increased with the level of external turbulence, similar to Wu & Faeth (1994). Legendre *et al.* (2006) simulated flow past a bubble and a solid sphere placed in turbulent pipe flow. The simulations were at low $Re = 200-500$, $u'_{ext}/U = 4\%$, and $l_{int}/D = O(10)$. The mean wake was found to decay as $U_0 \sim x^{-2}$, faster than the wake decay in all previous studies, when the streamwise distance ($x/D > 13$ for the sphere) became sufficiently large. This effect was attributed to a crossover point when the evolving defect velocity decreased to the same order as r.m.s of external turbulent fluctuations and a supporting theoretical analysis was provided. Different from the aforementioned studies, Amoura *et al.* (2010) elected to consider external turbulence with $l_{int}/D = O(1)$ while, similar to previous work, they con-

Case	$\frac{u'_{ext}}{U}$	$Re_{\lambda,ext}$	$\frac{L_{int,ext}}{L_{int,cl}}$	$\frac{L_{int,cl}}{2r_0}$
1. $EXT0_{unst}$	-	-	-	2.07
2. $EXT1_{unst}$	1%	≈ 88	≈ 4.03	2.07
3. $EXT3_{unst}$	3%	≈ 150	≈ 4.08	2.07
4. $EXT4_{unst}$	4%	≈ 181	≈ 4.44	2.07

Table 1. Parameters of the simulations. The r.m.s of external fluctuations varies between zero to 4% of the freestream mean velocity. The integral length scale is estimated as $L_{int} = K^{3/2}/\varepsilon$, and the initial ratio of its external value, $L_{int,ext}$, to that at the wake centerline, $L_{int,cl}$, is kept O(4). The microscale Reynolds number of the external freestream turbulence, $Re_{\lambda,ext} = \frac{20}{3}(\frac{k^2}{\varepsilon\nu})^{1/2}$ is moderate. Here, k and ε are the turbulent kinetic energy and dissipation rate, respectively. All simulations were performed with $N_1 = 2048$, $N_2 = 1024$ and $N_3 = 1024$ grid points in the x_1 (streamwise), x_2 (spanwise) and x_3 (vertical) directions, respectively. $L_1 = 81.92$, $L_2 = 40.96$ and $L_3 = 40.96$ are the computational domain lengths normalized by the body diameter.

sidered $Re = 100 - 1000$. High intensity turbulence was generated by a series of jets upstream of a water channel and the sphere, placed on the axis of the channel, was exposed to approximately homogeneous, isotropic turbulence with $u'_{ext}/U = 15 - 26\%$. The wake deficit velocity became smaller than the free-stream velocity by $x/D = 3$ and was found to subsequently exhibit $U_0 \sim x^{-2}$ scaling, much earlier than in the lower-intensity turbulence case of Legendre *et al.* (2006). Furthermore, Amoura *et al.* (2010) found that the r.m.s of external turbulence (it did not axially decay over the range of measurements) was the appropriate normalization velocity scale for similarity profiles and not the defect velocity.

Rind & Castro (2012*b*) experimentally studied the behavior of the axisymmetric disc wakes under the influence of free-stream turbulence. They found an augmentation in the drag owing to the presence of free-stream turbulence which leads to an increase in the wake deficit which in turn changes the decay rate of the far wake and therefore the approach to self-similarity is prevented. In a companion study (Rind & Castro (2012*a*)), direct numerical simulations (DNS) were performed in a triply periodic domain in which a self-similar wake was combined with various intensities of Saffman-type decaying homogeneous isotropic turbulence. They concluded that the wake departs from its self-similar behavior and the decay rate of the wake is augmented under the influence of the external turbulence.

More recently, Pal & Sarkar (2015) performed simulations to study the effect of the external turbulence on the evolution of the wake in both unstratified and stratified environments. The effect of background turbulence was discussed using visualizations, turbulence statistics and analysis of the *t.k.e* (turbulent kinetic energy) balance equation. External turbulence induced a faster decay of the mean wake in both unstratified and stratified wakes. For a given intensity of external turbulence, the stratified cases showed a stronger relative change of mean velocity. The parameter, u'_{ext}/u'_{cl}, which measures the intensity of the external turbulence relative to wake turbulence was found to play a key role. There was a rapid increase in the mean wake decay when u'_{ext}/u'_{cl} exceeded a value of approximately unity. Turbulence is entrained into the wake and the increase in cumulative shear production of turbulent kinetic energy augments the transfer from mean to turbulent fields, increasing the decay of the mean velocity.

The primary focus of this study is to understand the effect of the external turbulence when it has a higher integral length scale than that of the wake turbulence. The intensities of the external turbulence and wake turbulence are kept similar to that of Pal & Sarkar (2015). The ratio of the length scales, $l_{int,ext}/l_{cl,ext}$ used in the simulations of Pal & Sarkar (2015); Rind & Castro (2012*a*) was approximately 1. However, in the atmosphere or in ocean there can be a wide variation in length scales, motivating the current simulations with a larger integral length scale, $l_{int,ext}/l_{cl,ext} \simeq 4$.

PROBLEM FORMULATION

The formulation and the numerical method are as in our earlier work (Brucker & Sarkar, 2010; Pal & Sarkar, 2015). The governing equations are the three-dimensional, unsteady Navier-Stokes equations. For the towed wake, we employ a temporally evolving model (streamwise periodicity is assumed) without including the body similar to that in previous studies (Gourlay *et al.*, 2001; Dommermuth *et al.*, 2002; Brucker & Sarkar, 2010; Diamessis *et al.*, 2011). The distance from the body in the laboratory frame of reference is equivalent to time in the temporal frame and can be calculated as $x = x_0 + Ut$, where U is the constant towing velocity of the sphere in the laboratory frame. The temporally evolving simulations assume initial data with a prescribed initial mean and *r.m.s.* velocity profile as discussed below and the subsequent flow evolution is computed.

Initialization

The initial mean velocity is given by

$$\langle u_1(r)\rangle = U_0 e^{\left(-\frac{1}{2}\left(\frac{r}{r_0}\right)^2\right)}, \tag{1}$$

where U_0 is the centerline defect velocity and $r_0 = D/2$. The initial value of U_0 is taken to be 0.11 corresponding to an initial distance behind the body of $x_0/D \approx 7$. The initial velocity fluctuations are generated as an isotropic solenoidal velocity field in spectral space satisfying the following spectrum,

$$E(k) = (k/k_0)^4 e^{-2(k/k_0)^2}, \tag{2}$$

where $k_0 = 4$. The fluctuating field is localized to the wake by multiplying it with the following function,

$$g(r) = a\left[1 + \left(\frac{r}{r_0}\right)^2\right] e^{-\frac{1}{2}\left(\frac{r}{r_0}\right)^2}, \tag{3}$$

where a is the amplitude, $r = \sqrt{x_2^2 + x_3^2}$ and $r_0 = 0.5$ is the normalization parameter. The choice of the function $g(r)$ (Dommermuth *et al.*, 2002; Brucker & Sarkar, 2010) is consistent with laboratory measurements of *r.m.s.*

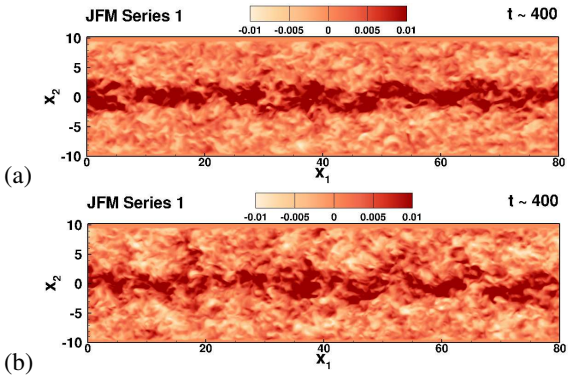

Figure 1. Contour plots of the instantaneous streamwise velocity in the horizontal (x_1 - x_2) plane at $t \approx 400$: (a) $EXT1_{unst}$ with $u'_{ext}/U = 1\%$; (b) $EXT4_{unst}$ with $u'_{ext}/U = 4\%$. Cases from Pal & Sarkar (2015) with $l_{int,ext}/l_{cl,ext} \simeq 1$.

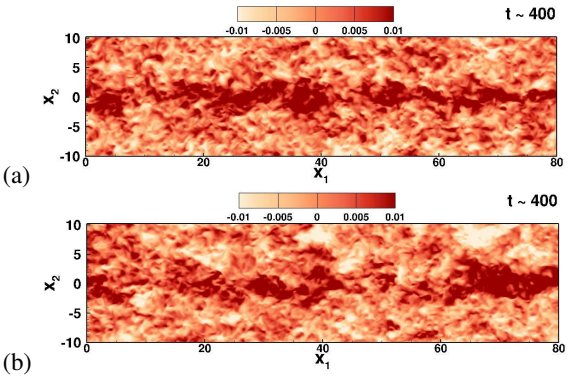

Figure 2. Contour plots of the instantaneous streamwise velocity in the horizontal (x_1 - x_2) plane at $t \approx 400$; (a) $EXT1_{unst}$; (b) $EXT4_{unst}$. Results from present cases with $l_{int,ext}/l_{cl,ext} \simeq 4$.

turbulence profiles, e.g. Bevilaqua & Lykoudis (1978). This initial fluctuating field is allowed to evolve, keeping the mean velocity profile given by (1) fixed until the maximum value of $\langle u'_1 u'_r \rangle / K \approx -0.25$, ensuring that the fluctuations establish a cross-correlation that is typical of turbulent shear flow. Here, K is the turbulent kinetic energy. Azimuthal and streamwise averaging are performed to obtain the time-evolving statistics during this adjustment period.

Equation (2) is employed to generate the initial level of background fluctuations but, instead of using the damping function (3) to localize the fluctuations to the wake, a case-dependent constant value is used for the amplitude a (a is chosen so as to obtain the required ratio of u'_{ext}/U). The pre-simulations for the external turbulence are performed in a triply periodic box and allowed to evolve as an isotropic turbulent field until the required ratio of u'_{ext}/U is achieved. The background turbulence decays as time advances in the simulations.

The external turbulent field is combined with the towed-wake in the outer region of the wake which, following Redford & Coleman (2007), is taken to be the region where the mean velocity of the towed wake is less than 5% of the maximum defect velocity. The combined field is allowed to adjust for a few time units to smear out the gradients that are initially generated at the interface between the two fields.

VISUALIZATION

We start the discussion by showing representative results from Pal & Sarkar (2015) who chose $l_{int,ext}/l_{cl,ext} \simeq 1$. Figure 1 shows contours of the streamwise velocity on a horizontal (x_1 - x_2) plane at time $t \approx 400$ for two cases with different levels of external turbulence. The 1% external turbulence case (figure 1(a)) shows little difference in the wake velocity with respect to the undisturbed background case (not shown). However, the 4% case shows that external turbulence distorts the wake and appears to broaden it somewhat. It was shown by Pal & Sarkar (2015), that fluctuations from the background were entrained into the flow and interacted with the wake leading to faster decay of the wake velocity in $EXT4_{unst}$ relative to $EXT0_{unst}$. Velocity fields from the present simulations are shown at the same time $t \approx 400$ in figure 2. At 1% level of external turbulence, there is already some influence on the wake evolution in the present simulation (figure 2(a)) in contrast to the corresponding case in figure 1(a). A detailed examination shows that the disintegration of the wake is stronger in the present cases as compared to the corresponding cases with the same initial turbulence level in series 1 of Pal & Sarkar (2015).

MEAN FLOW CHARACTERISTICS

Figure 3 shows the effect of external turbulence on the evolution of mean centerline defect velocity and contrasts this effect between the present simulations and our previous study (Pal & Sarkar, 2015). The center line defect velocity, U_0, under the influence of external turbulence (cases $EXT1_{unst}$, $EXT3_{unst}$ and $EXT4_{unst}$) decays faster than the undisturbed background case $EXT0_{unst}$ in Figure 3. We find a similar behavior in the mean kinetic energy integrated over the wake half-width (not shown). The evolution of the defect velocity for $EXT0_{unst}$ and $EXT1_{unst}$ are similar until $t \approx 90$. After $t \approx 90$, the defect velocity $EXT1_{unst}$ starts decaying faster in comparison to the undisturbed background case $EXT0_{unst}$. Cases $EXT3_{unst}$ and $EXT4_{unst}$, however show an earlier deviation from $EXT0_{unst}$ at $t \approx 40$. Interestingly, cases $EXT3_{unst}$ and $EXT4_{unst}$ evolve similarly without much difference between themselves.

TURBULENCE CHARACTERISTICS

Figure 4 shows profiles of the turbulent kinetic energy ($t.k.e.$) as a function of the spanwise direction x_2 at three different times for the present cases in the first column ((a), (c) and (e)) and the series 1 cases of Pal & Sarkar (2015) in the second column ((b), (d) and (f)). At time $t \approx 30$, we observe that the $t.k.e.$ for the cases with external turbulence with intensities of 3% and 4% are significantly higher outside the wake region and the transition from the wake to the external turbulence regime is very sharp as depicted in

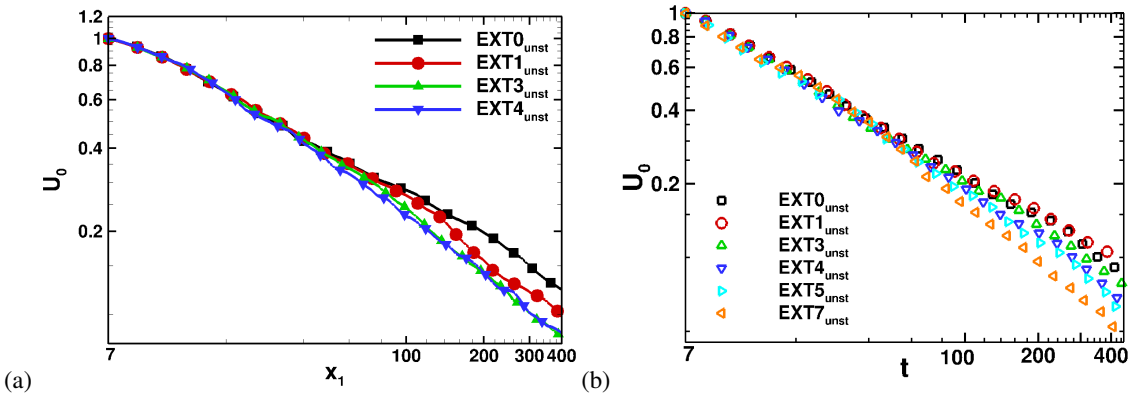

Figure 3. Mean defect velocity at $(x_2 = 0, x_3 = 0)$: (a) Present cases; (b) Cases from Pal & Sarkar (2015).

figure 4 (a). At the same time, the results of Pal & Sarkar (2015) (figure 4 (b)) show that the $t.k.e.$ for intensities of 3% and 4% has lower values external to the wake relative to corresponding values in figure 4 (a). Furthermore, there is a smooth transition from turbulence inside the wake to the external turbulence region in the previous study. However, $EXT7_{unst}$ in the *previous* study (figure 4 (b)) has higher external values of $t.k.e$ relative to inside the wake, analogous to the behavior of the $EXT3_{unst}$ and $EXT4_{unst}$ in the *present* simulations (figure 4 (a)). The $t.k.e.$ values in figure 4 (d) for the cases $EXT3_{unst}$ and $EXT4_{unst}$ are similar, but again $EXT7_{unst}$ has higher $t.k.e.$ explaining the substantially faster decay of the mean defect velocity in $EXT7_{unst}$ relative to the other case that was demonstrated earlier in figure 3 (b). The external $t.k.e.$ at $t \approx 90$ (figure 4 (e)) has decayed sufficiently in cases $EXT3_{unst}$ and $EXT4_{unst}$ of the present simulations so that the $t.k.e.$ profiles eventually show a smaller bump when passing from the wake to the background. The profile of $t.k.e.$ remains flat for cases $EXT3_{unst}$ and $EXT4_{unst}$ in the previous study after $t \approx 30$ and, although the level of $t.k.e.$ in case $EXT7_{unst}$ is larger than the other cases, the profile of $t.k.e.$ is also flat after $t \approx 60$.

The reason for longer survival of the external turbulence in the present simulations in comparison to the cases of Pal & Sarkar (2015) is the larger value of initial length scale ratio $L_{int,ext}/L_{int,cl}$ of approximately 4 as compared to the near-unity values in Pal & Sarkar (2015). The eddy turnover time scale scale is given by

$$\tau = \frac{K}{\varepsilon} = \frac{L_{int}}{K^{1/2}}\,, \tag{4}$$

where the integral length scale is taken here to be the large-eddy length scale, $K^{3/2}/\varepsilon$. Cases in the present simulations with the same value of external $t.k.e$ as in Pal & Sarkar (2015) have larger L_{int} and therefore larger turnover time scale, τ, leading to slower decay of external turbulence that was demonstrated in figure 4. Thus, the cumulative entrainment of external turbulence into the wake is larger relative to the previous study, leading to a stronger effect on the wake. We have also compared (but not plotted) the profiles of L_{int}/D among the different cases simulated here. At early time, all the cases with background fluctuations have a much larger value of L_{int} compared to that in the wake. With increasing time, L_{int} decreases throughout the flow but with a rate that is smaller in the wake. By $t \simeq 30$, the difference between background and wake values of L_{int} is substantially reduced for $EXT3_{unst}$ and $EXT4_{unst}$ and, by $t \simeq 60$, there is little difference.

CONCLUSIONS

The effect of external (background) turbulence on the evolution of a turbulent far wake has been investigated using direct numerical simulation of a temporally evolving wake at $Re = 10{,}000$. The external fluctuations are unforced and they decay in time as does the wake. It is found that, under the influence of background turbulence, the mean wake decays faster. The simulations are performed for a situation where the external turbulence has a larger integral length scale relative to wake turbulence. In particular, $L_{int,ext}/L_{int,cl} \simeq 4$ while our previous study (Pal & Sarkar, 2015) had $L_{int,ext}/L_{int,cl} \simeq 1$. We find that, even with a low intensity of $u^{'}_{ext}/U = 1\%$, the wake defect velocity is affected noticeably. The effect at 3% initial external turbulence level is as strong as that at 7% level in our previous study. The reason for this difference is the external turbulence, owing to larger length scale in the present cases, has a larger eddy-turnover time scale and a slower decay rate relative to the simulations of Pal & Sarkar (2015). The infiltration of the external turbulence into the wake continues for a relatively longer time owing to the survival of the external turbulence for a longer period, leading to the stronger cumulative effect on the wake when the initial $L_{int,ext}/L_{int,cl} \simeq 4$ instead of unity.

In Pal & Sarkar (2015), external turbulence was able to substantially affect the wake evolution only when the initial value of $u^{'}_{ext}/u^{'}_{cl} > 1$. In the present study, even when the initial value of $u^{'}_{ext}/u^{'}_{cl}$ is appreciably lower than unity, there is still a substantial effect on the wake because the wake turbulence decays faster than the external turbulence so that, soon into its evolution, the value of $u^{'}_{ext}/u^{'}_{cl}$ in the flow becomes comparable to unity as shown by figure 5.

REFERENCES

Amoura, Z., Roig, V., Risso, F. & Billet, A.M. 2010 Attenuation of the wake of a sphere in an intense incident turbulence with large length scales. *Phys. Fluids* **22**, 055105.

Bagchi, P & Balachandar, S 2004 Response of the wake of

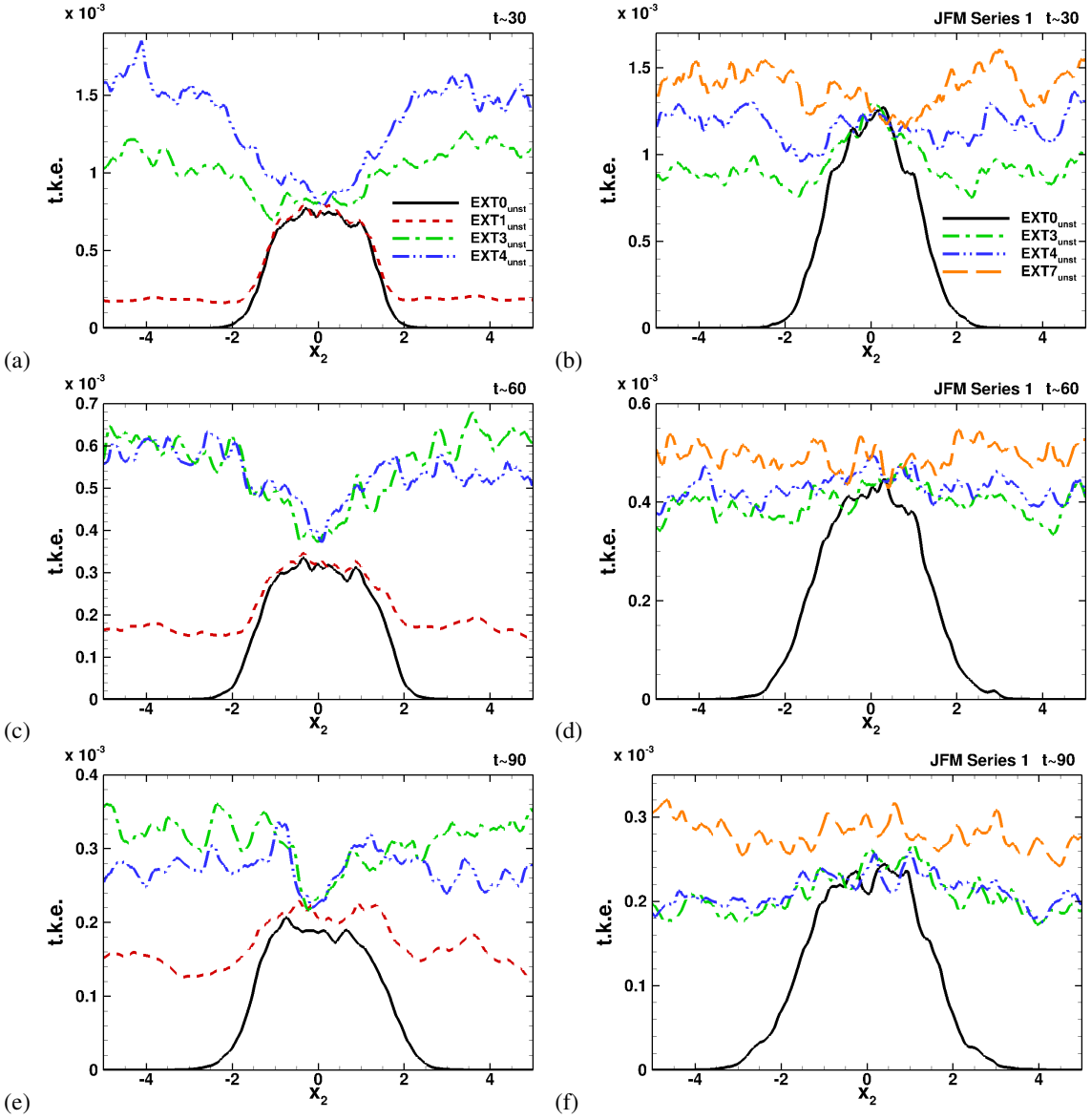

Figure 4. Profiles of the $t.k.e.$ vs x_2: (a) $t \approx 30$; (b) $t \approx 30$, from Pal & Sarkar (2015); (c) $t \approx 60$; (d) $t \approx 60$, from Pal & Sarkar (2015); (e) $t \approx 90$; (f) $t \approx 90$, from Pal & Sarkar (2015).

an isolated particle to an isotropic turbulent flow. *J. Fluid Mech.* **518** (1), 95–123.

Bevilaqua, P. M. & Lykoudis, P. S. 1978 Turbulence memory in self-preserving wakes. *J. Fluid Mech.* **89** (3), 589–606.

Brucker, K. A. & Sarkar, S. 2010 A comparative study of self-propelled and towed wakes in a stratified fluid. *J. Fluid Mech.* **652**, 373–404.

Diamessis, P. J., Spedding, G. R. & Domaradzki, J. A. 2011 Similarity scaling and vorticity structure in high Reynolds number stably stratified turbulent wakes. *J. Fluid Mech.* **671**, 52–95.

Dommermuth, D. G., Rottman, J. W., Innis, G. E. & Novikov, E. A. 2002 Numerical simulation of the wake of a towed sphere in a weakly stratified fluid. *J. Fluid Mech.* **473**, 83–101.

Gourlay, M. J., Arendth, S. C., Fritts, D. C. & Werne, J. 2001 Numerical modeling of initially turbulent wakes with net momentum. *Phys. Fluids A* **13**, 3783–3802.

Johansson, P. B. V., George, W. K. & Gourlay, M. J. 2003 Equilibrium similarity, effects of initial conditions and local reynolds number on the axisymmetric wake. *Phys. Fluids* **15**, 603.

Legendre, D, Merle, A & Magnaudet, J 2006 Wake of a spherical bubble or a solid sphere set fixed in a turbulent environment. *Phys. Fluids* **18**, 048102.

Pal, A. & Sarkar, S. 2015 Effect of external turbulence on the evolution of a wake in stratified and unstratified environments. *J. Fluid Mech.* **772** (361-385).

Redford, J.A. & Coleman, G.N. 2007 Numerical study of turbulent wakes in background turbulence. *5th International Symposium on Turbulence and Shear Flow Phenomena (TSFP-5 Conference), Munich, Germany,* pp. 561–566.

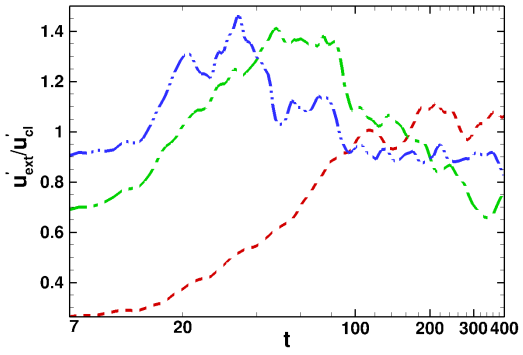

Figure 5. Evolution of the ratio of the external r.m.s streamwise fluctuation to the corresponding value at the centerline.

Redford, J. A., Castro, I. P. & Coleman, G. N. 2012 On the universality of turbulent axisymmetric wakes. *J. Fluid Mech.* **710**, 419.

Rind, E. & Castro, I. P. 2012*a* Direct numerical simulation of axisymmetric wakes embedded in turbulence. *J. Fluid Mech.* **710**, 482.

Rind, E. & Castro, I. P. 2012*b* On the effects of free-stream turbulence on axisymmetric disc wakes. *Exp. Fluids* **53** (2), 301–318.

Uberoi, M. S. & Freymuth, P. 1970 Turbulent energy balance and spectra of axisymmetric wake. *Phys. Fluids* **13** (9), 2205–2210.

Wu, J-S & Faeth, G. M. 1994 Sphere wakes at moderate Reynolds numbers in a turbulent environment. *AIAA J.* **32** (3), 535–541.

Wu, J-S & Faeth, G. M. 1995 Effect of ambient turbulence intensity on sphere wakes at intermediate Reynolds number. *AIAA J.* **33** (1), 171–173.

Wygnanski, I., Champagne, F. & Marasli, B. 1986 On the large-scale structures in two-dimensional, small-deficit, turbulent wakes. *J. Fluid Mech.* **168** (1), 31–71.